THE JOURNAL OF PHYSICAL CHEMISTRY B

 VOLUME 108, NUMBER 40, OCTOBER 7, 2004

LETTERS

Internal Ceramic Reconstruction Weakens Metal−ZrO_2 Adhesion

Juan I. Beltrán, Silvia Gallego, Jorge Cerdá, J. Serafín Moya, and M. Carmen Muñoz*

Instituto de Ciencia de Materiales de Madrid, CSIC, 28049 Cantoblanco, Madrid, Spain

Received: July 5, 2004; In Final Form: August 3, 2004

The mechanisms that control at the quantum level the adhesion of metals to ZrO_2 are studied on the basis of density functional theory calculations of the Ni/c-ZrO_2 interface. Our results indicate that the interface fragility is inherently connected to the ability of the ceramic matrix to locally reconstruct from the stabilized cubic structure toward the more stable low temperature phases. We consider with special detail the impact on the metal−ceramic bonding of the O vacancies and dopants that actually exist in the oxide lattice. Whereas vacancies greatly reduce the adhesion, the presence of dopants of large atomic volume such as Y inhibit the reconstruction of the ceramic, reinforcing the metal−ceramic bonds.

Cermets, the combination of a ceramic matrix and metal particles, are multifunctional materials widely applied in a large diversity of fields, from chirurgical implants to coatings of nuclear reactors.[1] A tremendous technological and research effort is consequently devoted to the improvement and control of the metal−oxide interface adhesion, critical for the proper performance of cermet-based devices. The addition of metal particles to ceramics is intended to increase the toughness of the ceramic matrix. Surprisingly, in the case of ZrO_2 this results in the fragility of the metal−ceramic bonds, as experimentally proved for metals such as Cu, Pd, or Ni.[2−4] Though pure zirconia is monoclinic (m-ZrO_2) at room temperature, most applications are based in the stabilized high-temperature phases, tetragonal (t-ZrO_2) and cubic (c-ZrO_2), where the Zr coordination to O increases from 7-fold to 8-fold. We will concentrate on cubic ZrO_2/Ni interfaces, one of the more promising oxide/metal combinations due to the good matching of the structural and thermal properties of both components. A first-principles study of thin ZrO_2 layers on a Ni(111) substrate[5] reports that the significant adherence found at the monolayer level decays for thicker ceramic films up to three layers. By contrast, in a more recent study of ideal Ni/c-ZrO_2(100) polar interfaces,[6] we found that they are thermodynamically stable, with a large work of separation (w). Our results predicted the formation of relatively strong chemical bonds at the interface, the reported O|Ni bond strength (BS) values being 5 times larger than those found in ref 5 for the three layers thick film. The fact that the authors of ref 5 employed a larger lateral unit cell as well as a "less constrained" slab geometry suggests that the number of degrees of freedom associated to the ceramic slab plays a key role in the O−Ni adherence. Our previous study of neutral O vacancies at the Ni/c-ZrO_2 interface[8] supports this idea: the existence of thermodynamic (neutral) O vacancies, present in ZrO_2 ceramics sintered in a reducing atmosphere,[7] relaxes the structural constraints in the zirconia lattice, favoring the local reconstruction to a monoclinic-like structure over the Ni−O interaction. To test this hypothesis, in this Letter we study at the quantum level the behavior of the O−Ni BS under different chemical and geometrical local environments.

We initially consider the symmetric slab depicted in Figure 1a, hereafter referred as V_0^{sym}, and relax its geometrical constraints by gradually breaking its symmetry. Note that V_0^{sym} is very similar to the slab employed in ref 6, although the thickness has been reduced due to computational limitations. First, we

* Corresponding author. E-mail: mcarmen@icmm.csic.es.

10.1021/jp047051t CCC: $27.50
Published on Web 09/15/2004

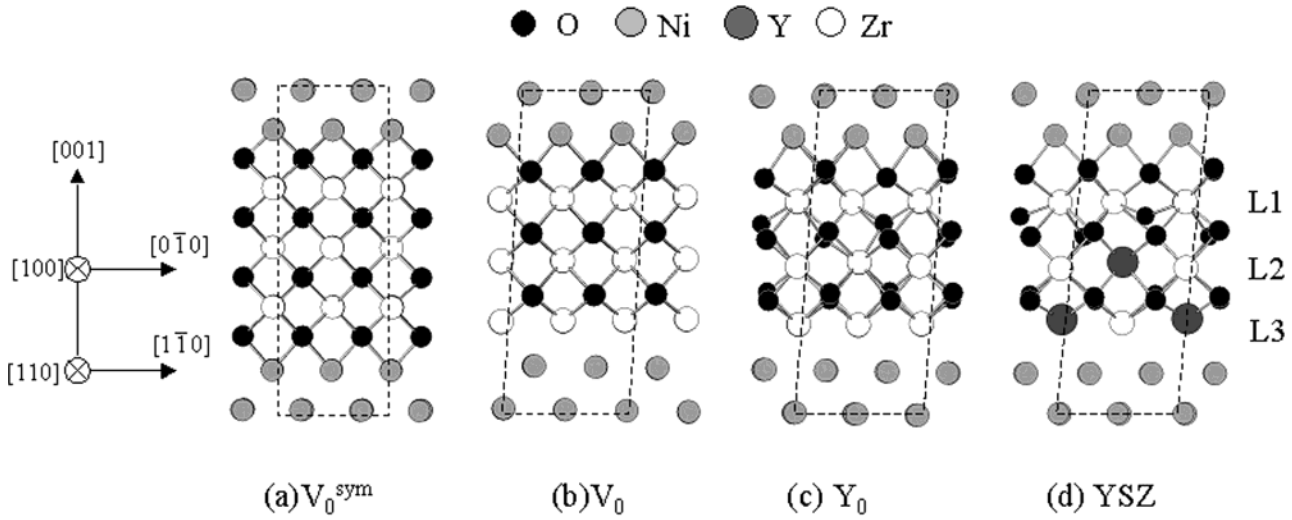

Figure 1. Side view of four of the relaxed ZrO_2 slabs under study. The cationic planes of the YSZ lattice are numbered as L1−3. The dashed lines indicate the supercell unit cell. The horizontal axes on the left refer to the ZrO_2 (upper) and Ni (bottom) lattices.

lift the mirror symmetry in the *z*-direction by considering an asymmetric slab where the oxygen layer has been removed at one of the interfaces (V_0, Figure 1b). Next, we also introduce in-plane relaxations at the ceramic slab by removing one O atom (i.e., generating a thermodynamic vacancy) at the O−Ni interface (Y_0, Figure 1c). Finally, we also consider the presence of yttria (Y_2O_3) dopants in the ceramic (Figure 1d). c-ZrO_2 is stabilized at low temperatures when doped with oxides such as Y_2O_3, so that the substitution of tetravalent Zr by lower valence cations is charge balanced by the formation of anion vacancies. For trivalent dopants such as Y, one oxygen ion is removed out of two dopant cations introduced in the ZrO_2 lattice. We model yttria-stabilized zirconia (YSZ) with a standard doping of 20% mol of yttria. Different studies of the local structure of YSZ have found that Y preferentially occupies next-nearest neighbors (N−NN) instead of NN sites to the vacancy;[9] thus, in our model the substitutional Y atoms are placed in the second and third Zr planes, while the O vacancy is kept at the interface. Intermediate situations between Y_0 and YSZ are also considered, retaining only one of the Y atoms either at the second (L2) or third (L3) cationic plane (see Figure 1); the corresponding structures are labeled Y_1^{L2} and Y_1^{L3}, respectively.

All calculations have been performed with the ab initio SIESTA code[10] based on the standard density functional method in the generalized gradient approximation (GGA).[11] Details on the computational conditions and parameters can be found elsewhere.[6] Despite the reduced thickness of the slabs, the results reproduce within less than 3% those obtained for thicker slabs of 5 layers in the absence of anion vacancies and Y_2O_3 dopants. Furthermore, bulklike behavior is already retrieved at the central layers of the metal and ceramic slabs. For all the structures of Figure 1 the Ni[100] and ZrO_2[110] crystallographic orientations are aligned, assuming a slight in-plane distortion of the Ni lattice to make it commensurate to the ZrO_2 slab. The Ni atoms are placed at bridge positions relative to the two-dimensional (2D) unit cell of ZrO_2, the most stable configuration for the defect-free (ideal) Ni|O interface.[6] For the nondefected slabs, V_0^{sym} and V_0, a perfect matching is assumed between a c(2×2) and a p(1×1) cell at the Ni and ZrO_2 slabs, respectively, whereas for the structures with O vacancies we double the cell size, employing a p(2×2) and a c(2×2) cell for the Ni and ZrO_2 slabs, respectively. A schematic illustration of the 2D primitive cell in the presence of vacancies is presented in Figure 2. All O atoms are 2-fold coordinated to Ni, which adopts two types

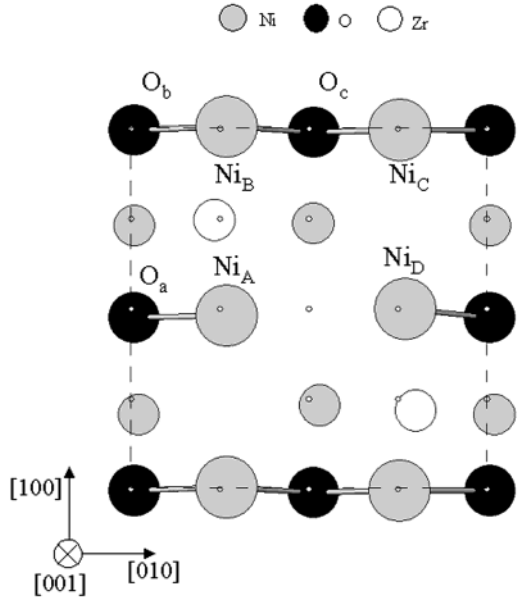

Figure 2. Top view of the relaxed O|Ni interface with O vacancies, including only the four atomic planes (two of Ni and two of ZrO_2) closest to the interface. As a reference, the ideal unrelaxed lattice sites are marked by small dots. The sizes of the atoms are set proportional to their distance to the interface. The O and Ni atoms at the interface plane are labeled according to the different sites of the 2D unit cell, also indicating the O−Ni interface bonds.

of sites at the interface: first, that of Ni_A and Ni_D, NN to the vacancy and 1-fold coordinated to oxygen; and second, the 2-fold O-coordinated Ni_B and Ni_C sites. For the ideal structures V_0^{sym} and V_0, only one Ni site can be distinguished, bonded to two O atoms similarly to $Ni_{B,C}$.

In Table 1 we give the *w* and average BS of the structures considered. The work of separation is defined as the difference in total energy between the assembled slab and that obtained introducing a large vacuum region at the O|Ni interface. Though *w* is a lower bound to the experimental work of adhesion,[12] it provides a direct measure of the interface BS, obtained by taking into account all NN's interactions. The most significant effect shown in the table is the dramatic decrease of the interface adhesion for Y_0. This evidences that increasing the degrees of freedom of the ceramic structure has a direct impact on the interface adhesion. As we move from V_0^{sym} to Y_0, there is a

TABLE 1: Works of Separation (mJ/m^2) and Bond Strengths for the O|Ni Interfaces of the Slabs under Study

slab	*w*	BS
V_0^{sym}	5632.06	1.19
V_0	4925.09	1.04
Y_0	1215.31	0.34
Y_1^{L3}	2156.29	0.61
Y_1^{L2}	3736.67	1.06
YSZ	4149.98	1.19

clear weakening of the metal-ceramic bonding. Notably, enhancing the presence of Y near the interface gradually restores the BS. For YSZ there is also a reduction of *w* but not of the BS, which indicates that the interface bonds are similar or even stronger than for V_0^{sym} and V_0, and that it is the reduced number of interface bonds induced by the O vacancy that leads to the final decrease in *w*.

As we will demonstrate here, these results are intimately related to the internal stability of the ceramic lattice. When bulk bonds are broken to form the interface, the oxide compensates the unbalanced charge either by binding to the adjacent Ni atoms or by an internal restructuring. For the cases V_0^{sym}, V_0, and YSZ, the inner bulk charges are in equilibrium, and the interface O atoms need the additional Ni cations to stabilize their valence state. On the contrary, when thermodynamic O vacancies exist, the unstable c-ZrO_2 structure has room to restructure toward the stable m-ZrO_2 phase, and this is preferred over the binding to Ni. In support of this, the intermediate situations represented by Y_1^{L2} and Y_1^{L3} are respectively more similar to the cases YSZ and Y_0, indicating that the proximity of the Y atom to the defected interface is relevant for the bonding. The validity of the above reasoning is evidenced by the structural and bond properties of the systems considered. The first hint comes from the equilibrium interface structures of Figure 1. They show that here the metal atoms do not segregate into the ceramic slab, contrary to other metal−ceramic interfaces with vacancies;[13] this has an effect on the bonding, as ref 13 reports a strong enhancement of the metal adhesion induced by the interface defects. The detailed analysis of the interface O−Ni distances confirms this idea. They are given, together with their corresponding average values, at the bottom left panel of Figure 3 for all structures under study. The variation of the mean bond distances between the different structures can be anticorrelated to that of the BS (see Table 1): the shorter the distance, the larger the BS. There is a significant dispersion of the individual interatomic values when O vacancies are present. This seems to confirm that, even if the global interface adhesion is reduced, some of the O−Ni bonds are weakened at the cost of reinforcing the others, in agreement with the results of ref 5. The top left panel of Figure 3 shows the O−Zr distances for the interface O atoms. Taking V_0^{sym} as reference, in all cases an enlarged O−Ni distance corresponds to a shortened O−Zr distance, implying that the O−Ni BS results from the interplay between the forward and back bonds of O. This indicates that ZrO_2 profits from the additional structural degrees of freedom to approach the low-temperature phases, where long and short O−Zr bonds coexist. (The 7-fold coordination unit of m-ZrO_2 contains three ranges of interatomic distances: below 2.10 Å, around 2.17 Å, and over 2.25 Å. Also t-ZrO_2 is characterized by two kind of Zr−O distances, about 2.40 and 2.05 Å.) In fact, a transition toward a monoclinic-like structure induced by the thermodynamic O vacancies was already described in detail in ref 8. The most significant variations of the bond lengths correspond to Y_0, where *w* drops dramatically. The situation is different in the presence of charged vacancies. The Y atoms, being larger than those of Zr, limit the magnitude of the atomic displacements, preventing a transition to more stable phases characterized by the wide range of O−Zr bond distances.

The right panels of Figure 3 show the bonding overlap populations (BOPs) of the interface O atoms with their Ni (bottom) and Zr (top) neighbors. They provide an estimate of the amount of hybridization of the bonding orbitals. In addition, the Mulliken populations of the corresponding atoms are given in Table 2. In general, for both the BOPs and charges there is a significant dispersion of the individual values at the defected interfaces, as previously observed for the interatomic distances. But clearly there is a uniform reduction of the mean O−Ni BOP as we move to Y_0 either from V_0^{sym} or from YSZ. This suggests

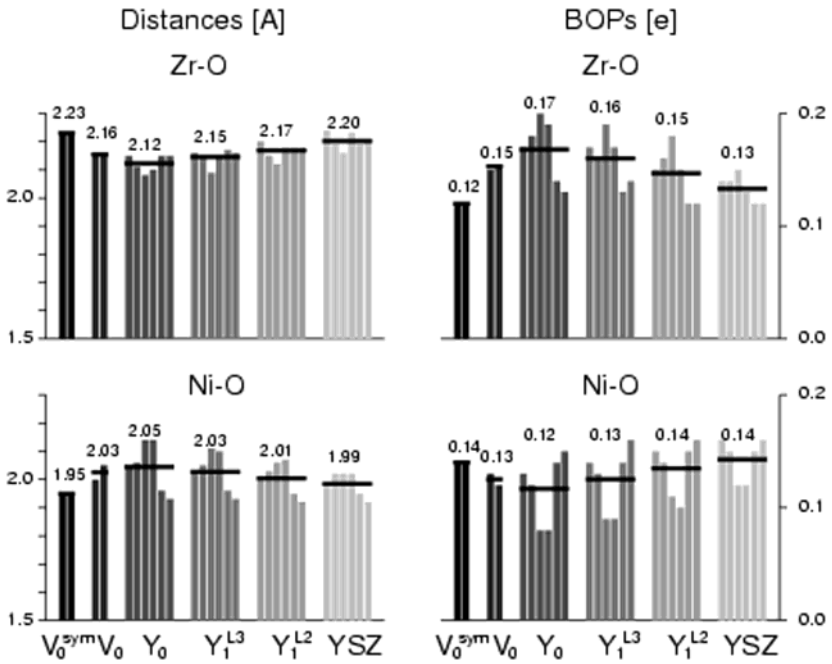

Figure 3. Bar diagrams showing the interatomic distances (Å) and BOPs between the interface O atoms and the adjacent (bottom) Ni and (top) Zr cations, for all slabs under study. Numbers and horizontal lines indicate the average value for each bar diagram.

TABLE 2: Mulliken Charges of the Ni, O, and Zr Atoms Closest to the O|Ni Interface for the Slabs under Study[a]

		V_0^{sym}	V_0	Y_0	Y_1^{L3}	Y_1^{L2}	YSZ
Q(Zr)	mean	2.42	2.48	2.59	2.58	2.56	2.55
		2.42	2.48	2.59	2.60	2.57	2.56
				2.59	2.55	2.54	2.53
Q(O)	mean	6.63	6.62	6.63	6.65	6.65	6.66
	a	6.62	6.62	6.64	6.65	6.65	6.66
	b			6.64	6.65	6.66	6.67
	c			6.62	6.64	6.65	6.66
Q(Ni)	mean	9.73	9.74	9.80	9.80	9.79	9.79
	A	9.73	9.74	9.85	9.85	9.84	9.83
	B			9.76	9.76	9.75	9.74
	C			9.75	9.75	9.74	9.73
	D			9.85	9.85	9.84	9.84

[a] The O and Ni sites for the interfaces with vacancies are labeled according to Figure 2.

a less covalent character of the O−Ni bonds in the presence of thermodynamic O vacancies. On the other hand, the Mulliken populations show a lower electron transfer from Ni to O as we approach to the situation of Y_0, indicating a reduced ionicity of the interface O−Ni bonds. The reduction of both the ionic and covalent character of the interface bonds implies their global weakening, as already evidenced by the interatomic distances. The same analysis of the BOPs and charges for the O−Zr pairs reveals higher hybridization and lower ionicity as we move to Y_0. This enhancement of the covalent character for the O−Zr bonds resembles the situation of the m-ZrO_2 structure, the stable phase at room temperature.

To summarize, the reduction of the structural constraints in metal/c-ZrO_2 interfaces leads to the internal restructuring of the ceramic slab to approach the low-temperature phases. The more the degrees of freedom, the larger the reconstruction, which in turn implies a stronger Zr−O interaction at the cost of weakening the interface bonds. This would explain the observed fragility of the metal−ceramic interface at these cermets. Among the defects inherent to the c-ZrO_2 structure, the O vacancies need special consideration. On one hand, they decrease the number of interface bonds, favoring a weakened adhesion. Moreover, in the absence of additional factors (i.e., for neutral vacancies) they induce the ceramic restructuring and actually lower the interface interaction. On the other hand, in the case of charged vacancies such as those in YSZ, the presence of the Y cationic dopants prevents the internal reconstruction of the ceramic, so that the Zr−O interaction cannot be strengthened and the interface BS is not actually reduced. Our results indicate that the metal−ceramic adhesion in ZrO_2 is not only an interface property, but it is governed by an internal ceramic tendency to locally set a stable bulk phase. In other words, intraceramic interactions prevail over metal−ceramic interactions, reducing the metal adhesion. A similar effect occurs in the martensitic phase transition from t-ZrO_2 to m-ZrO_2: the reduced constraints in the ceramic grains act to increase the resistance of the ceramic to crack propagation. In conclusion, the present study proves that the metal/c-ZrO_2 interface fragility is inherent to the ability of the ceramic to locally reconstruct from the cubic phase to the structures stable at low temperatures.

Acknowledgment. This work has been partially financed by the Spanish Ministerio de Ciencia y Tecnología and DGICyT under contracts MAT2003-04278 and MAT2001-1596. J.I.B. acknowledges financial support from the I3P program of the CSIC.

References and Notes

(1) (a) Choudhary, V. R.; Uphade, B. S.; Pataskar, S. G. *Appl. Catal., A* **2002**, *227*, 29. (b) Sinnott, S. B.; Dickey, E. C. *Mater. Sci. Eng. R* **2003**, *43*, 1, and references therein.

(2) (a) Duh, J. G.; Chien, W. S.; Chiou, B. S. *J. Mater. Sci. Lett.* **1989**, *8*, 405. (b) Qin, C.-D.; James, N. A.; Derby, B. *Acta Metall. Mater.* **1992**, *40*, 925.

(3) López-Esteban, S.; Bartolomé, J. F.; Moya, J. S.; Tanimoto, *J. Mater. Res.* **2002**, *17*, 1592.

(4) (a) Sotiropoulou, D.; Ladas, S. *Surf. Sci.* **1998**, *408*, 182. (b) Harel, S.; Mariot, J.-M.; Hague, C. F. *Surf. Sci.* **1992**, *269−270*, 1167.

(5) Christensen, A.; Carter, E. A. *J. Chem. Phys.* **2001**, *114*, 5816.

(6) Beltrán, J. I.; Gallego, S.; Cerdá, J.; Moya, J. S.; Muñoz, M. C. *Phys. Rev. B* **2003**, *68*, 075401.

(7) Zhu, W. Z.; Yan, M. *J. Mater. Sci. Lett.* **1997**, *16*, 1540.

(8) Beltrán, J. I.; Gallego, S.; Cerdá, J.; Muñoz, M. C. *J. Eur. Ceram. Soc.* **2003**, *23*, 2737.

(9) (a) Bogicevic, A.; Wolverton, C.; Crosbie, G.M.; Stechel, G. M. *Phys. Rev. B* **2001**, *64*, 014106. (b) Bogicevic, A.; Wolverton, C. *Phys. Rev. B* **2003**, *67*, 024106.

(10) (a) Ordejón, P.; Artacho, E.; Soler, J. M. *Phys. Rev. B* **1996**, *53*, R10441. (b) Soler, J. M.; Artacho, E.; Gale, J. D.; García, A.; Junquera, J.; Ordejón, P.; Sánchez-Portal, D. *J. Phys.: Condens. Matter* **2002**, *14*, 2745.

(11) Perdew, J. P.; Chevary, J. A.; Vosko, S. H.; Jackson, K. A.; Pederson, M. R.; Singh, D. J.; Fiolhais, C. *Phys. Rev. B* **1992**, *46*, 6671.

(12) Finnis, M. W. *J. Phys.: Condens. Matter* **1996**, *8*, 5811.

(13) Zhukovskii, Y. F.; Kotomin, E. A.; Jacobs, P. W. M.; Stoneham, A. M. *Phys. Rev. Lett.* **2000**, *84*, 1256.